




BRIEF DEFINITIVE REPORT

Selective inhibition of low-affinity memory CD8⁺ T cells by corticosteroids

Akihiro Tokunaga^{1,2*}, Daisuke Sugiyama^{3*}, Yuka Maeda^{1*}, Allison Betof Warner^{4,5} , Katherine S. Panageas⁶, Sachiko Ito³, Yosuke Togashi¹, Chika Sakai¹, Jedd D. Wolchok^{4,5} , and Hiroyoshi Nishikawa^{1,3} 

Patients treated with immune checkpoint blockade (ICB) sometimes experience immune-related adverse events (irAEs), requiring immuno-suppressive drugs such as corticosteroids despite the possibility that immunosuppression may impair the antitumor effects of ICB. Here, we address the dilemma of using corticosteroids for the treatment of irAEs induced by ICB. ICB augments neoantigen-specific CD8⁺ T cell responses, resulting in tumor regression. In our model, simultaneous, but not late, administration of corticosteroids impaired antitumor responses with reduction of CD8⁺ T cell proliferation. Secondary challenge using tumors with/without the neoantigen showed selective progression in tumors lacking the neoantigen when corticosteroids were administered. Corticosteroids decreased low- but not high-affinity memory T cells by suppressing fatty acid metabolism essential for memory T cells. In a small cohort of human melanoma patients, overall survival was shorter after treatment with CTLA-4 blockade in patients who received early corticosteroids or had low tumor mutation burden. Together, low-affinity memory T cells are dominantly suppressed by corticosteroids, necessitating careful and thoughtful corticosteroid use.

Introduction

Cancers use several immune inhibitory mechanisms including decreased expression of relevant antigens and major histocompatibility complex-class I molecules resulting in the failure of CD8⁺ T cells to recognize cancer cells, increased expression of various immunosuppressive molecules, and induction/recruitment of immunosuppressive cells (e.g., myeloid-derived suppressor cells, tumor-associated macrophages, and regulatory T cells), impairing the development of antitumor immune responses (Pitt et al., 2016; Chen and Mellman, 2017). Full engagement of antitumor immune responses could enable the host to regain control of tumor growth. Cancer immunotherapy in the form of immune checkpoint blockade (ICB), including anti-cytotoxic T lymphocyte-associated antigen-4 (CTLA-4) antibody (Ab) and anti-programmed cell death 1 (PD-1) Ab, reactivates cytotoxic T cells and facilitates killing of cancer cells, providing significant clinical efficacy across various types of cancer, even in patients with advanced disease (Khalil et al., 2016; Palucka and Banchereau, 2016).

CTLA-4 down-regulates costimulatory immune signaling and delivers an inhibitory signal during immune responses (Leach et al., 1996; Eisenstein et al., 2016). CTLA-4 is expressed by activated T cells and regulatory T cells. It is up-regulated after TCR stimulation and is known to suppress a broad range of immune responses (Wing and Sakaguchi, 2010). Blockade of CTLA-4 action by mAb augments effector T cell responses, resulting in T cell-mediated tumor rejection in preclinical mouse models and human cancer patients (Leach et al., 1996; Hodi et al., 2010). PD-1 is also a negative immune modulator that inhibits both TCR and costimulatory signals and is expressed following activation of T cells (Freeman et al., 2000; Hui et al., 2017; Kamphorst et al., 2017). While the expression of PD-1 is rapidly down-regulated after acute antigen stimulation, chronic stimulation (such as viral infections and malignancies) induces high PD-1 expression (Wherry and Kurachi, 2015). PD-1 blockade elicits strong antitumor T cell responses and is widely used a variety of cancers (Khalil et al., 2016; Palucka and Banchereau, 2016; Kamphorst et al., 2017).

¹Division of Cancer Immunology, Research Institute/Exploratory Oncology Research and Clinical Trial Center, National Cancer Center, Kashiwa, Japan; ²Oncology Research and Development Unit, Kyowa Kirin Co., Ltd., Shizuoka, Japan; ³Department of Immunology, Nagoya University Graduate School of Medicine, Nagoya, Japan; ⁴Parker Institute for Cancer Immunotherapy, Swim Across America-Ludwig Collaborative Lab, Memorial Sloan-Kettering Cancer Center, New York, NY; ⁵Weill Cornell Medical College, New York, NY; ⁶Departments of Epidemiology and Biostatistics, Memorial Sloan Kettering Cancer Center, New York, NY.

*A. Tokunaga, D. Sugiyama, and Y. Maeda contributed equally to this paper; Correspondence to Hiroyoshi Nishikawa: hnishika@ncc.go.jp; Jedd D. Wolchok: wolchokj@MSKCC.ORG.

© 2019 Tokunaga et al. This article is distributed under the terms of an Attribution–Noncommercial–Share Alike–No Mirror Sites license for the first six months after the publication date (see <http://www.rupress.org/terms/>). After six months it is available under a Creative Commons License (Attribution–Noncommercial–Share Alike 4.0 International license, as described at <https://creativecommons.org/licenses/by-nc-sa/4.0/>).

Since immune checkpoint molecules are also involved in self-tolerance and maintenance of immune homeostasis, ICB can potentiate immune responses against self-antigens and cause a spectrum of symptoms reminiscent of autoimmune disorders (June et al., 2017). Treatment with anti-CTLA-4 or anti-PD-1 mAb is therefore complicated by concomitant immune-related adverse events (irAEs), including skin rash, gastrointestinal inflammation, and hypophysitis (Hodi et al., 2010; Callahan et al., 2016; June et al., 2017). Management of irAEs often requires immunosuppressive drugs such as corticosteroids, but these medications have the potential to suppress antitumor immune responses elicited by ICB. Reassuringly, clinical experience to date has not revealed an obvious deleterious effect of immune suppression for irAE treatment on the clinical activity of ICB (Horvat et al., 2015). Therefore, detailed mechanisms of immune suppression by corticosteroids need to be clarified in order to better understand this apparent uncoupling of tumor immunity from autoimmunity. Deeper insight into these mechanisms could improve irAE management with corticosteroids, especially as new immunotherapy agents and combinations emerge in the clinic that have the potential additional or novel irAEs (Wolchok et al., 2017).

In this study, we address the challenge of using immunosuppressive drugs for the treatment of irAEs induced by ICB. Dosage and timing of corticosteroids are key mediators of the antitumor efficacy of ICB. Therefore, clinicians should use corticosteroids carefully and thoughtfully when treating irAEs in order to balance toxicity management with clinical benefit from ICB.

Results and discussion

We first investigated the impact of corticosteroids on antitumor immune responses elicited by CTLA-4 blockade using animal models. BALB/c mice were inoculated with CMS5a with stable expression of a model tumor neoantigen NY-ESO-1 (CMS5a-NY-ESO-1; Nishikawa et al., 2006) and treated with anti-CTLA-4 mAb (Fig. 1 A). CTLA-4 blockade induced complete tumor regression in >90% of mice (Fig. 1, B and C). Methylprednisolone was administered beginning on the same day as anti-CTLA-4 mAb treatment as in Fig. 1 A, because in some patients with symptomatic brain tumors, such as those with glioblastoma and malignant melanoma, corticosteroids are required to be given concurrently with ICB. Dosing of corticosteroids was selected based on human equivalent dose; low-dose corticosteroids was 20 μg per mouse (0.7–1 $\mu\text{g}/\text{g}$) and high-dose corticosteroids was 2,000 μg per mouse (67–110 $\mu\text{g}/\text{g}$), which is thought to represent a pulse steroid dose (Feng et al., 2017). Early administration of corticosteroids induced a dose-dependent reduction in NY-ESO-1-specific CD8⁺ T cells in tumors treated with anti-CTLA-4 mAb; CMS5a-NY-ESO-1 tumor progression was not controlled in 40% of mice treated with corticosteroids and anti-CTLA-4 mAb (Fig. 1, B–D), consistent with a previous report of impaired T cell activation by corticosteroids (Löwenberg et al., 2007). Ki-67 expression by NY-ESO-1-specific CD8⁺ T cells was decreased by corticosteroids in a dose-dependent manner (Fig. S1 A), though PD-1/Tim-3 expression (Fig. S1 B) and IFN- γ /TNF- α

production (Fig. S1 C) were not changed, indicating that corticosteroids mainly inhibited the proliferation of antigen-specific CD8⁺ T cells, but effector functions remained intact. In the clinical setting, irAEs are sometimes accompanied by tumor regression. To reflect this, corticosteroids were injected after tumors started regressing in response to CTLA-4 blockade (Fig. 1 E). In this setting, neither low- nor high-dose corticosteroid administration reduced antitumor activity by anti-CTLA-4 mAb (Fig. 1, F and G), indicating that late administration of corticosteroids has limited influence on efficacy of this therapy. Similar results were observed in another tumor model, CT26 with stable expression of NY-ESO-1 (CT26-NY-ESO-1; Fig. S1, D and E) and with anti-PD-L1 mAb as an alternative ICB (Fig. 2, A–F).

In mice treated with early corticosteroids, even at a low dose, some animals experienced regrowth of the tumor after initial tumor regression (Fig. 1 C). Although not frequent enough to achieve statistical significance, this observation suggests that early corticosteroids may inhibit memory CD8⁺ T cells that are involved in durable antitumor responses (Butler et al., 2011). We then asked whether memory T cell differentiation was influenced by corticosteroids. Mice that had completely eradicated the initial tumors after anti-CTLA-4 mAb with or without early corticosteroid treatment (Fig. 1 C) were secondarily challenged with CMS5a-NY-ESO-1 cells (right hind flank) and parental CMS5a cells (left hind flank; Fig. 3 A). Almost all mice rejected the CMS5a-NY-ESO-1 cells regardless of corticosteroid treatment (Fig. 3 B). The growth of parental CMS5a was delayed in anti-CTLA-4 mAb-treated mice, but this tumor growth inhibition was abrogated in mice treated with both low- and high-dose corticosteroids (Fig. 3 C), indicating the possible inhibition of memory T cells recognizing nondominant antigens. Similar results were observed in the CT26-NY-ESO-1 model (Fig. S1 F) and with anti-PD-L1 mAb treatment (Fig. S1 G).

Since memory precursor effector cells (MPECs) generate long-lived CD8⁺ memory T cells (Joshi et al., 2007), we analyzed the proportion of MPECs in tumor tissues. These cells reportedly express high levels of CD127 and low levels of KLRG1. When anti-CTLA-4 mAb and corticosteroids were administered as in Fig. 1 A, activated CD8⁺CD69⁺ T cells in CMS5a-NY-ESO-1 tumors were separated into NY-ESO-1-tetramer⁺ and NY-ESO-1-tetramer⁻ populations (Fig. 3 D). The TCR repertoires of NY-ESO-1-tetramer⁻CD8⁺CD69⁺ T cells in CMS5a-NY-ESO-1 tumors were comparable with those of CD8⁺CD69⁺ T cells infiltrating into parental CMS5a tumors (Fig. S2, A and B), confirming that this NY-ESO-1-tetramer⁻CD8⁺CD69⁺ T cell fraction included effector CD8⁺ T cells responding to antigens presented by parental CMS5a cells. Moreover, higher expression of T-bet was observed in the NY-ESO-1-tetramer⁺CD69⁺ population compared with the NY-ESO-1-tetramer⁻CD69⁺ population (Fig. S2 C), indicating that the NY-ESO-1-tetramer⁺CD69⁺ population had higher affinity TCRs than the NY-ESO-1-tetramer⁻CD69⁺ population, given that T-bet expression reportedly increases depending on TCR affinity (Knudson et al., 2013). To further confirm the differences in TCR affinity of NY-ESO-1-specific CD8⁺ T cells and CD8⁺ T cells specific for internal tumor antigens of CMS5a cells, we performed a comparative analysis of the levels of phosphorylated TCR signaling

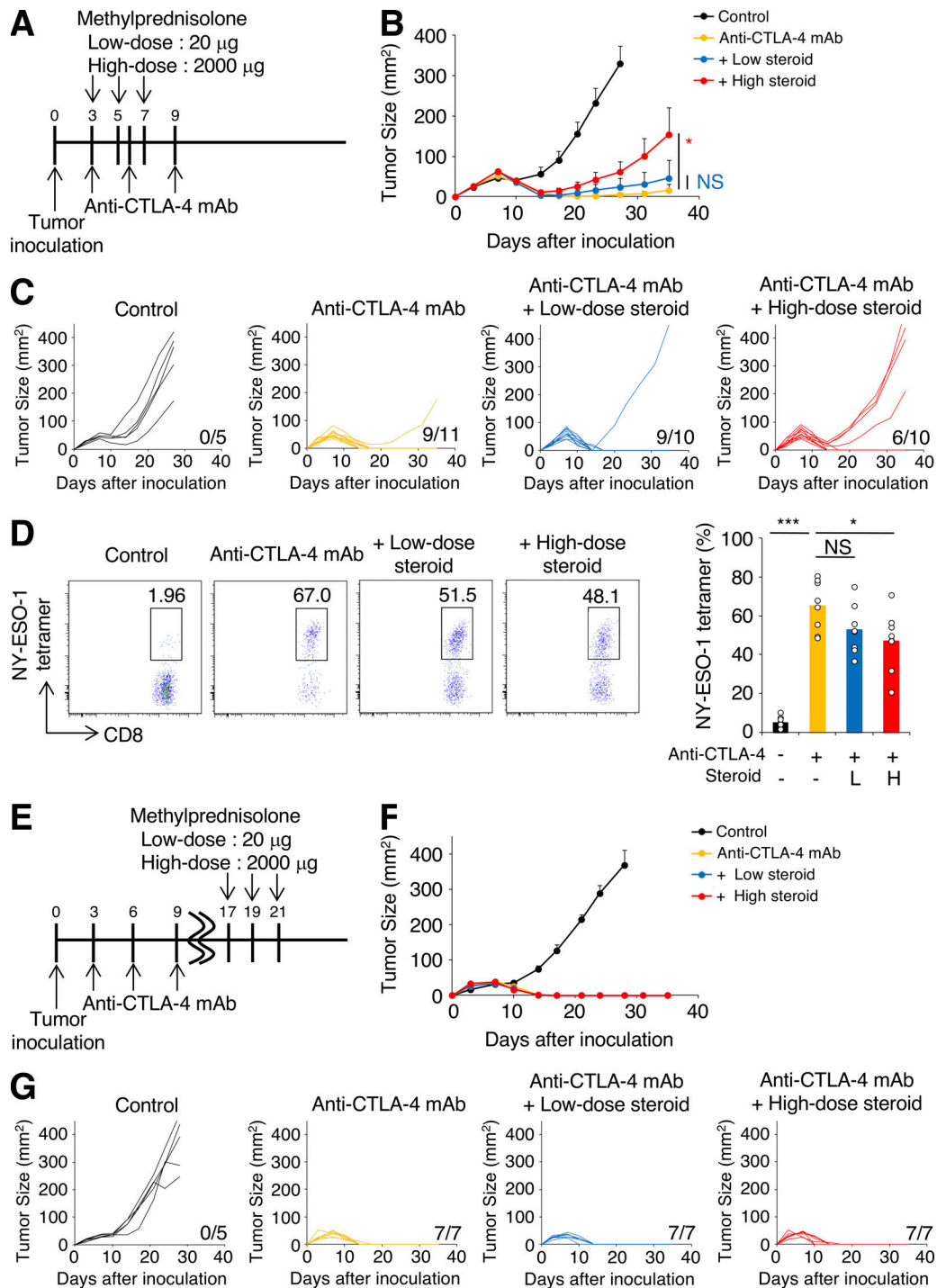


Figure 1. Early corticosteroid treatment reduces antitumor activity by anti-CTLA-4 mAb in a dose-dependent fashion. (A–C) Experimental schema (A) and tumor growth curves (B: mean, C: individual mice) of early corticosteroid treatment. BALB/c mice were inoculated with CMS5a-NY-ESO-1 and injected with anti-CTLA-4 mAb on days 3, 6, and 9 after tumor inoculation. Corticosteroid administration was started on the same day with anti-CTLA-4 mAb ($n = 5–11$). **(D)** Representative flow cytometric analysis (left) and summary (right) of NY-ESO-1-tetramer⁺CD8⁺ T cells in CMS5a-NY-ESO-1 tumors at 10 d after tumor inoculation ($n = 8$). L, low dose; H, high dose. **(E–G)** Experimental schema (E) and tumor growth curves (F: mean; G: individual mice) of late corticosteroid treatment. BALB/c mice were inoculated with CMS5a-NY-ESO-1 and injected with anti-CTLA-4 mAb on days 3, 6, and 9 after tumor inoculation. Corticosteroid administration was started on day 17 ($n = 5–7$). Data in B and F are mean + SE. Statistical analysis by Dunnett’s test; *, $P < 0.05$; ***, $P < 0.001$. These experiments were performed independently three times with similar results.

molecules (ZAP-70 and ERK1/2) and IFN- γ production. CMS5a tumors reportedly have an internal tumor antigen (CMS5a-intAg) recognized by T cells with the highest immunogenicity

(Hanson et al., 2000). Mice were immunized with NY-ESO-1 peptide (RGPE SRL) or CMS5a-intAg peptide (QYIHSANVL), and NY-ESO-1-specific or CMS5a-intAg-specific CD8⁺ T cells

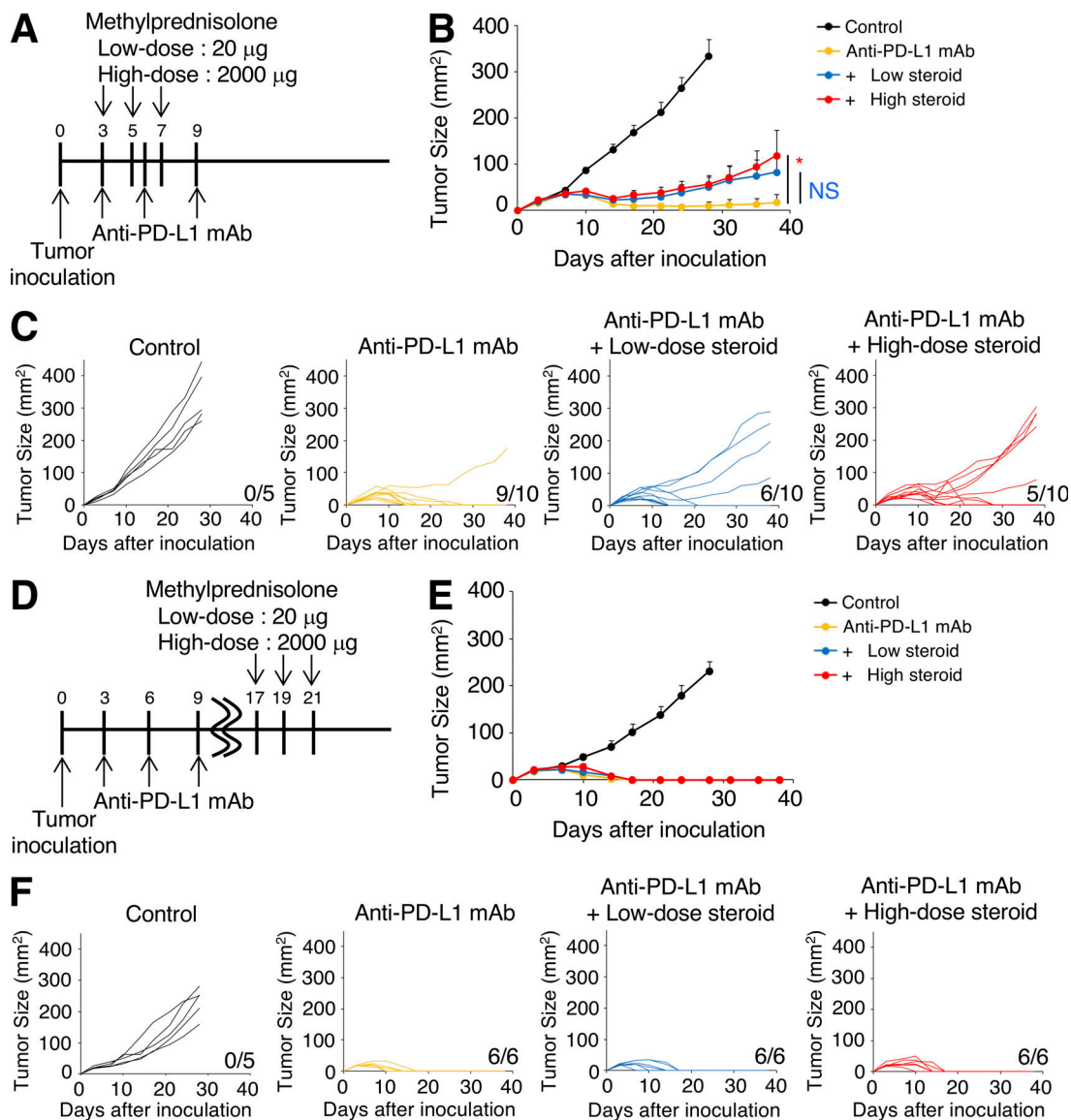


Figure 2. Early corticosteroid treatment reduces antitumor activity by anti-PD-L1 mAb. (A–C) Experimental schema (A) and tumor growth curves (B: mean; C: individual mice) of early corticosteroid treatment. BALB/c mice were inoculated with CT26-NY-ESO-1 and injected with anti-PD-L1 mAb on days 3, 6, and 9 after tumor inoculation. Corticosteroid administration was started on the same day of anti-PD-L1 mAb ($n = 5–10$). **(D–F)** Experimental schema (D) and tumor growth curves (E: mean; F: individual mice) of late corticosteroid treatment. BALB/c mice were inoculated with CT26-NY-ESO-1 and injected with anti-PD-L1 mAb on days 3, 6, and 9 after tumor inoculation. Corticosteroid administration was started on day 17 ($n = 5$ or 6). Data in B and E are mean \pm SE. Statistical analysis by Student's t test; *, $P < 0.05$. These experiments were performed independently three times with similar results.

were prepared from local draining lymph nodes. The levels of p-ZAP-70, p-ERK1/2, and IFN- γ production in NY-ESO-1-specific CD8 $^+$ T cells were significantly higher than those in CMS5a-intAg-specific CD8 $^+$ T cells (Fig. S2, D and E). In IFN- γ production by ELISPOT assay, a model tumor neoantigen NY-ESO-1 provided a far stronger TCR signal than any intrinsic CMS5a antigens (Fig. S2 F). Together, the model tumor neoantigen NY-ESO-1-specific (NY-ESO-1-tetramer $^+$ CD8 $^+$ CD69 $^+$) and non-NY-ESO-1 reactive (NY-ESO-1-tetramer $^-$ CD8 $^+$ CD69 $^+$) T cells could be used to represent high-affinity foreign-derived and low-affinity self-derived antigen-specific T cells, respectively. Whereas MPECs in high-affinity CD8 $^+$ T cells in CMS5a-NY-ESO-1 tumors were not affected by corticosteroids, the proportion of

MPECs in low-affinity CD8 $^+$ T cells was significantly decreased (Fig. 3, E and F), suggesting selective suppression of memory T cells depending on TCR affinity. While a model in which T cells are unresponsive to corticosteroids may be useful to reveal the effect of corticosteroids, glucocorticoid-receptor antisense transgenic mice have abnormal thymic development of T cells (Ashwell et al., 2000; Löwenberg et al., 2007) and may not be suitable for investigation of memory T cell generation. Therefore, we chose to study detailed mechanism(s) via comprehensively exploring actual T cell responses in wild-type mice.

We then investigated the possibility of corticosteroid mediating immune suppression via effects on dendritic cell (DC)

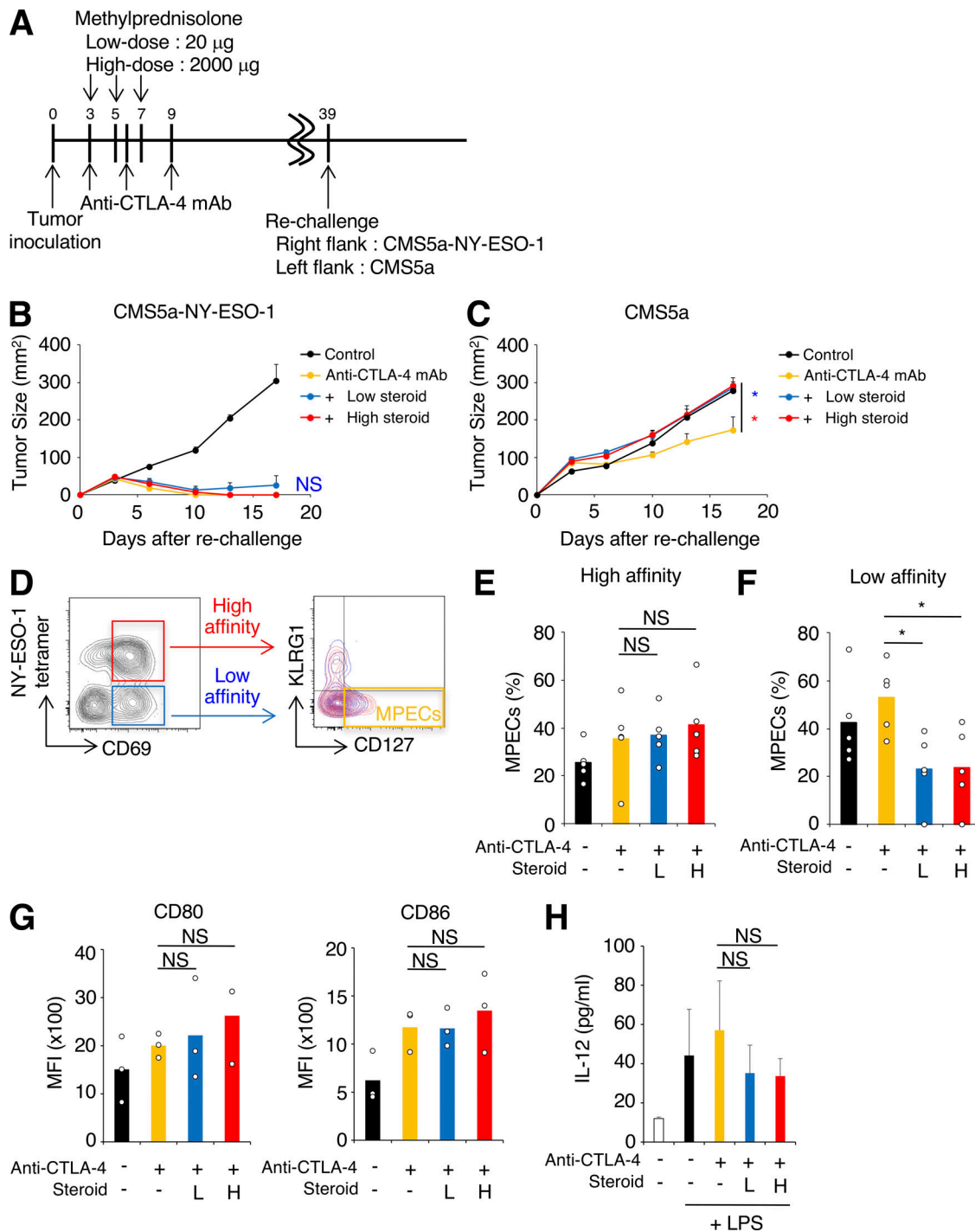


Figure 3. Early corticosteroid treatment impairs low-affinity memory T cell differentiation. (A–C) Experimental schema (A) and tumor growth curves (B: CMS5a-NY-ESO-1; C: CMS5a) of rechallenge to early corticosteroid-treated mice. CMS5a-NY-ESO-1-bearing mice were treated as in Fig. 1 A. Mice that had completely rejected the initial tumors were collected and secondarily inoculated with CMS5a-NY-ESO-1 and parental CMS5a (day 39). Control naive mice were injected with the same tumors ($n = 5-10$). **(D)** Gating strategy for flow-cytometric analysis of MPECs population in high-affinity (NY-ESO-1-tetramer⁺) and low-affinity (NY-ESO-1-tetramer⁻) CD8⁺ T cells at 10 d after tumor inoculation. **(E and F)** Percentages of MPECs in high- (E) and low-affinity (F) CD8⁺ T cells ($n = 5$). L, low dose; H, high dose. **(G)** Expression of maturation markers on DCs (CD11c⁺MHC class II⁺CD8a⁺) in tumor-draining lymph nodes 10 d after tumor inoculation ($n = 3$). MFI, mean fluorescence intensity. **(H)** Cytokine production (IL-12p70) by DCs. DCs from draining lymph nodes in CMS5a-NY-ESO-1-bearing mice were stimulated with LPS overnight. Cytokine production was measured by ELISA ($n = 3$ or 4). Data in B, C, and H are mean + SE. Statistical analysis by Dunnett's test; *, $P < 0.05$. These experiments were performed independently three times with similar results.

maturation. CD8 α^+ DCs present exogenous antigens to CD8 $^+$ T cells by cross presentation, eliciting CD8 $^+$ T cell activation and memory T cell differentiation (Hildner et al., 2008; Scholer et al., 2008). Additionally, human tumor-associated and tumor-draining lymph node DCs and macrophages highly express PD-L1 and suppress antitumor immunity (Curiel et al., 2003; Lin et al., 2018). Expression of maturation markers of CD8 α^+ DCs was not altered by corticosteroids (Fig. 3 G). In addition, production of cytokines such as IL-12p70 was not changed by corticosteroids (Fig. 3 H), indicating that corticosteroids likely inhibit memory T cell generation directly, rather than by inhibiting DC maturation and function.

To address the differential sensitivity of T cells to corticosteroids depending on their TCR affinity, we employed OT-I TCR transgenic CD8 $^+$ T cells in which graded TCR signaling can be delivered with different peptides such as the high-affinity peptide SIINFEKL (N4) or the low-affinity peptide SIYNFEKL (Y3; Zehn et al., 2009). OT-I cells stimulated with N4 or Y3 were treated with various concentrations of corticosteroids in vitro, and the proportion of OVA-specific CD8 $^+$ T cells was determined. Activation of OVA-specific CD8 $^+$ T cells was impaired by adding corticosteroids in a dose-dependent manner, particularly in OT-I cells stimulated with Y3 (Fig. 4 A), indicating that low-affinity T cells were more sensitive to corticosteroids.

Corticosteroids cause immune suppression in part by nuclear translocation of the glucocorticoid receptor (GR; Barnes and Adcock, 2009). The GR is phosphorylated by the MAPK pathway via ERK1/2 and JNK, and this phosphorylation attenuates nuclear translocation of the GR after engaging corticosteroids and regulation of transcription of target genes (Barnes and Adcock, 2009). Therefore, corticosteroid activity is partially dependent on MAPK activation status. Phosphorylation levels of ZAP-70, ERK1/2, and JNK were higher in N4-primed OT-I cells compared with Y3-primed cells, in accordance with their TCR affinity (Fig. 4 B), indicating that the N4 (high-affinity) peptide provided far stronger TCR signals compared with the Y3 (low-affinity) peptide. Antigen abundance did not have the same effect on phosphorylation levels, as levels of phosphorylated ZAP-70, ERK1/2, and JNK plateaued in >1 nmol/liter peptide (Fig. 4 B). Accordingly, GR in N4-primed OT-I cells also were highly phosphorylated compared with that in Y3-primed OT-I cells (Fig. 4 C). As corticosteroid sensitivity seemed to be proportional to the strength of TCR signaling, we employed an anti-CD3 mAb to explore the generalizability of this phenomenon. When naive CD8 $^+$ T cells were stimulated with titrated doses of anti-CD3 mAb, higher levels of phosphorylated ERK1/2, JNK, and GR were observed proportional to the dose of anti-CD3 mAb (Fig. S3, A and B). Further, the phosphorylation level of GR was also significantly higher in NY-ESO-1-specific CD8 $^+$ T cells than CMS5a-intAg-specific CD8 $^+$ T cells in the peptide-immunized mouse model (Fig. S3 C). Together, these findings suggest that low-affinity T cells are more sensitive to corticosteroids than high-affinity T cells due to their lower phosphorylation of GR.

To further gain insight into the mechanism(s) underlying selective inhibition of low-affinity T cells by corticosteroids, we examined the target genes for corticosteroids by investigating gene expression in OT-I cells stimulated with N4 or Y3 peptide

with or without corticosteroids. Gene-set enrichment analysis (GSEA) revealed significant enrichment of genes involved in fatty acid metabolism in corticosteroid-untreated Y3- but not in N4-primed OT-I cells, compared with comparable cells treated with corticosteroid (Fig. 4 D and Fig. S3 D), while other signature sets of genes were not significantly changed, indicating that fatty acid metabolism was down-regulated only in corticosteroid-treated low-affinity T cells. Because fatty acid oxidation (FAO) is essential for CD8 $^+$ memory T cell development (Pearce et al., 2009; van der Windt et al., 2012), we focused on the effect of corticosteroids on FAO. Y3-primed OT-I cells treated with corticosteroids had less expression of FAO-regulated genes than control Y3-primed OT-I cells, but this was not the case in N4-primed cells (Fig. 4 E; and Fig. S3, E and F). Similar results were also observed with CD8 $^+$ T cells treated with high- and low-dose anti-CD3 mAb (Fig. S3 G).

FAO can be assessed by cellular oxygen consumption after adding an inhibitor of CPT1a, which transports long chain fatty acids into mitochondria and is the rate-limiting enzyme of FAO (van der Windt et al., 2012). Consistent with low expression of FAO-regulated genes, FAO was significantly impaired by corticosteroids in Y3-primed OT-I cells and low-dose anti-CD3 mAb-stimulated CD8 $^+$ T cells, but not in N4-primed or high-dose anti-CD3 mAb-stimulated cells (Fig. 4 F and Fig. S3 H). We further examined whether corticosteroid administration suppressed FAO-regulated gene expression in low-affinity T cells in vivo. In accordance with the in vitro data, low-affinity but not high-affinity T cells in CMS5a-NY-ESO-1 tumors treated with corticosteroids also showed markedly less FAO-regulated gene expression and decreased mitochondrial function associated with FAO (Fig. 4, G and H). Thus, corticosteroids suppressed FAO in low-affinity T cells due to their lower levels of phosphorylated GR, resulting in impaired memory T cell differentiation. Since FAO-regulated genes reportedly are not direct targets of GR, corticosteroids may control these genes indirectly through regulating other transcription factors such as CCAAT/enhancer binding protein β ; expression of this transcription factor is repressed by activated GR and regulates FAO (Wang et al., 2004, 2008; Ki et al., 2005; Phuc Le et al., 2005). Yet it is controversial whether FAO is essential for memory T cell development, as a recent study showed that CPT1a deletion did not affect memory T cell development (Raud et al., 2018). Genetic depletion of CPT1a may induce the activation of alternative pathway not generally used because of the critical role of FAO in memory T cell generation. Future studies focused on the relationship between FAO and memory T cell development are warranted.

To examine the influence of corticosteroids on the clinical activity of ICB in cancer patients, we analyzed 86 patients with malignant melanoma who were treated with the anti-CTLA-4 mAb ipilimumab (Fig. 5 A). When the timing of corticosteroid administration was considered, overall survival (OS) was slightly shorter in patients who received corticosteroids within the first 7 wk of ipilimumab treatment than in patients who did not receive corticosteroids (Fig. 5 B). When the data were analyzed by which patients received corticosteroids in the first 16 wk of ipilimumab treatment, slightly longer, though not

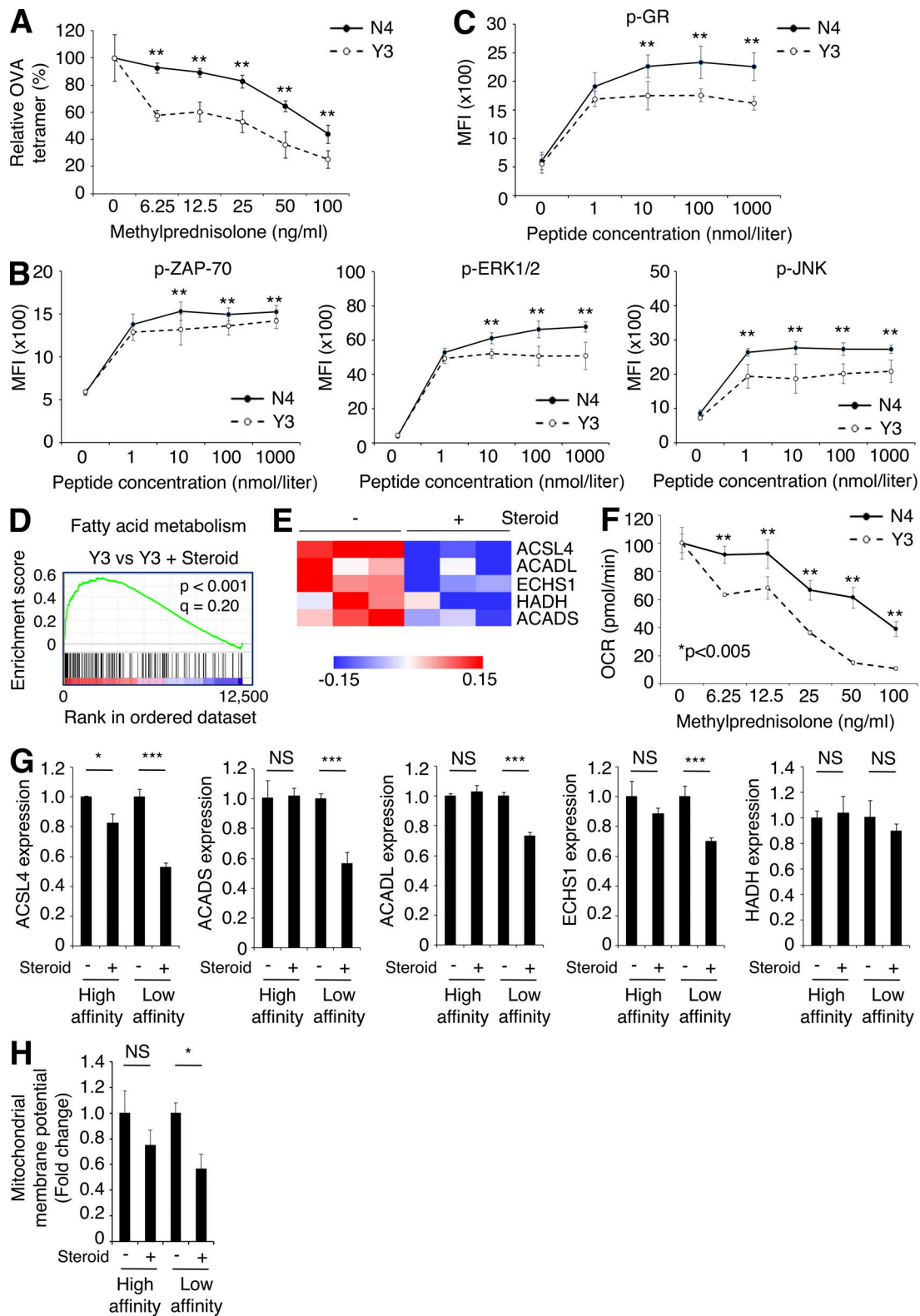


Figure 4. Corticosteroids compromise FAO in low-affinity but not high-affinity memory T cells. (A) Relative frequency of OVA tetramer⁺ cells. OT-I cells were stimulated with N4 (high-affinity) or Y3 (low-affinity) peptide, and treated with various concentrations of corticosteroids in vitro. Frequency of OVA tetramer⁺ CD8⁺ T cells on day 7 was determined. The graph shows the percentage of OVA tetramer⁺ cells in CD8⁺ T cells in comparison with the control culture without corticosteroids (n = 3). (B) Quantitative analysis of TCR signaling. OT-I cells were stimulated with various concentrations of N4 or Y3 peptide for 3 h. Phosphorylation of ZAP-70 (left), ERK1/2 (middle), and JNK (right) was determined by flow cytometry (n = 5). MFI, mean fluorescence intensity. (C) Phosphorylation of GR. OT-I cells were stimulated with various concentrations of N4 or Y3 peptide for 3 h. Phosphorylation of GR was determined by flow cytometry (n = 5). (D) GSEA of fatty acid metabolism-related genes in Y3 stimulated OT-I cells relative to those treated with corticosteroids. (E) Heat map of expression of

FAO-related genes. OT-I cells were stimulated with Y3 peptide and treated with corticosteroids in vitro for 4 d. mRNA expression was examined with microarray. **(F)** OCR of peptide-stimulated OT-I cells with etomoxir. OT-I cells were stimulated with N4 or Y3 peptide, and treated with various concentrations of corticosteroids in vitro for 4 d. FAO was determined with etomoxir by measuring OCR using extracellular flux analyzer ($n = 5$). **(G)** FAO-related mRNA expression in high- or low-affinity CD8⁺ T cells in CMS5a-NY-ESO-1 tumors at 10 d after tumor inoculation ($n = 3$). **(H)** FAO-associated mitochondrial membrane potential in high- or low-affinity CD8⁺ T cells in CMS5a-NY-ESO-1 tumors at 10 d after tumor inoculation ($n = 4$). Data in A–C and F–H are mean \pm SD. Statistical analysis by Student's *t* test; *, $P < 0.05$; **, $P < 0.01$; ***, $P < 0.001$. These experiments were performed independently three times with similar results.

significant, OS was seen compared with patients who did not receive corticosteroids (Fig. 5 B). This suggests that late corticosteroid treatment may be associated with a better therapeutic outcome than early treatment.

Our preclinical data suggest that low-affinity memory T cells are more sensitive to corticosteroids than high-affinity memory T cells. CD8⁺ T cells that recognize immunogenic foreign antigens (such as neoantigens stemming from gene mutations in cancer cells) generally have a higher-affinity TCR than CD8⁺ T cells specific for self-antigens (Yarchoan et al., 2017). It follows that the CD8⁺ T cells that recognize mutational neoantigens could therefore be resistant to corticosteroids. Consequently, patients with tumors containing a high-mutation burden showed a significantly better prognosis compared with those with a low-mutation burden with bivariate Cox model (>22 mutation burden, hazard ratio 0.21 [95% CI 0.07–0.62] $P = 0.004$; used steroids, hazard ratio 0.62 [95% CI 0.31–1.28] $P = 0.20$). We then performed subgroup analyses of patients treated with corticosteroids either early (≤ 7 wk) or late (> 7 wk) and those with high (>22) vs. low (≤ 22) mutational burden, for whom information on mutation burden and clinical course were available. While no clinical impact of corticosteroid administration was observed in patients with segregated by high- or low-mutation burden, patients with a low-mutation burden who were treated with corticosteroids at an early time point had a significantly worse prognosis than patients who received corticosteroids later (Fig. 5, C–F). In contrast, no significant differences were observed between early and late corticosteroid treatment in patients with high-mutation burden (Fig. 5, C–E and G). Together, this implies that corticosteroid administration dampens the antitumor effects by anti-CTLA-4 mAb depending on the timing of corticosteroid administration and tumor mutation burden. We recognize that the modest size and uncontrolled nature of the clinical data from this single-institution dataset with long follow-up make this finding hypothesis-generating. Future studies with large patient cohorts treated with ICB and combinations are therefore warranted for confirmation.

Given that neoantigen-specific CD8⁺ T cells with high-affinity TCR are important for the antitumor effects of ICB, it is possible that corticosteroid administration could be optimized to control autoimmunity induced by self-antigen-specific CD8⁺ T cells that generally harbor low-affinity TCRs without affecting tumor neoantigen-specific high-affinity CD8⁺ T cells (Yarchoan et al., 2017). However, reduction of memory T cells by corticosteroids might inhibit objective and durable antitumor responses by ICB (Butler et al., 2011). It is well known that tumor antigens are mainly classified into two categories, tumor-specific antigens including neoantigens and tumor-associated

antigens including shared-antigens (Van den Eynde and van der Bruggen, 1997). TCR generally engage with higher affinity to tumor-specific antigens than tumor-associated antigens (Yarchoan et al., 2017). One can speculate that corticosteroids have little effect on antitumor responses by ICB in cancer patients with a large number of neoantigens recognized by T cells with high-affinity TCR. On the other hand, when corticosteroids are required in cancer patients with few neoantigens, antitumor effects may be dampened. In fact, corticosteroid-treated patients harboring malignant melanomas with low-mutation burden had poorer outcomes than similar patients with high-mutation burden. Therefore, it is important to consider the potential impairment of memory T cells when administering corticosteroids for irAEs. We assessed the effect of corticosteroids on T cells and APCs due to the critical roles of CD8⁺ T cells in the ICB-mediated antitumor response (Khalil et al., 2016). Yet as corticosteroids influence various cell types, additional studies are needed to better define other potential effects of corticosteroids.

In conclusion, we provide evidence that corticosteroids inhibit antitumor efficacy of ICB in a dose- and timing-dependent manner. Additionally, low- but not high-affinity memory T cells specific to self-antigens are dominantly suppressed by corticosteroids mainly by inhibition of FAO. Therefore, the type of tumor antigens recognized by T cells and neoantigen burden could be key factors regarding whether corticosteroid usage affects the antitumor response to ICB. Furthermore, well-timed usage of corticosteroids has the potential to selectively control autoimmunity without negatively impacting antitumor immunity. Additional clinical studies with large cohorts are warranted to determine the appropriate timing and dosage of corticosteroid treatment as well as other interventions for irAEs (e.g., TNF blockade, mycophenolate mofetil).

Materials and methods

Cell line and mice

CMS5a is a subcloned cell line obtained from CMS5, a 3-methylchoranthrene-induced sarcoma cell line of BALB/c origin. CMS5a-NY-ESO-1 is a cell line derived from CMS5a stably transfected with NY-ESO-1 (Nishikawa et al., 2006). CT26 is a colon epithelial tumor cell line derived by intrarectal injections of N-nitroso-N-methylurethane in BALB/c mice (Griswold and Corbett, 1975). CT26-NY-ESO-1 is a cell line derived from CT26 stably transfected with NY-ESO-1 (Mitsui et al., 2010). P1.HTR is a subline of P815 mastocytoma cell line of DBA/2 origin (Nishikawa et al., 2006). CMS5a, CMS5a-NY-ESO-1, CT26, CT26-NY-ESO-1, and P1.HTR were maintained in RPMI1640 supplemented with 10% FBS and 4 mmol/liter of L-glutamine.

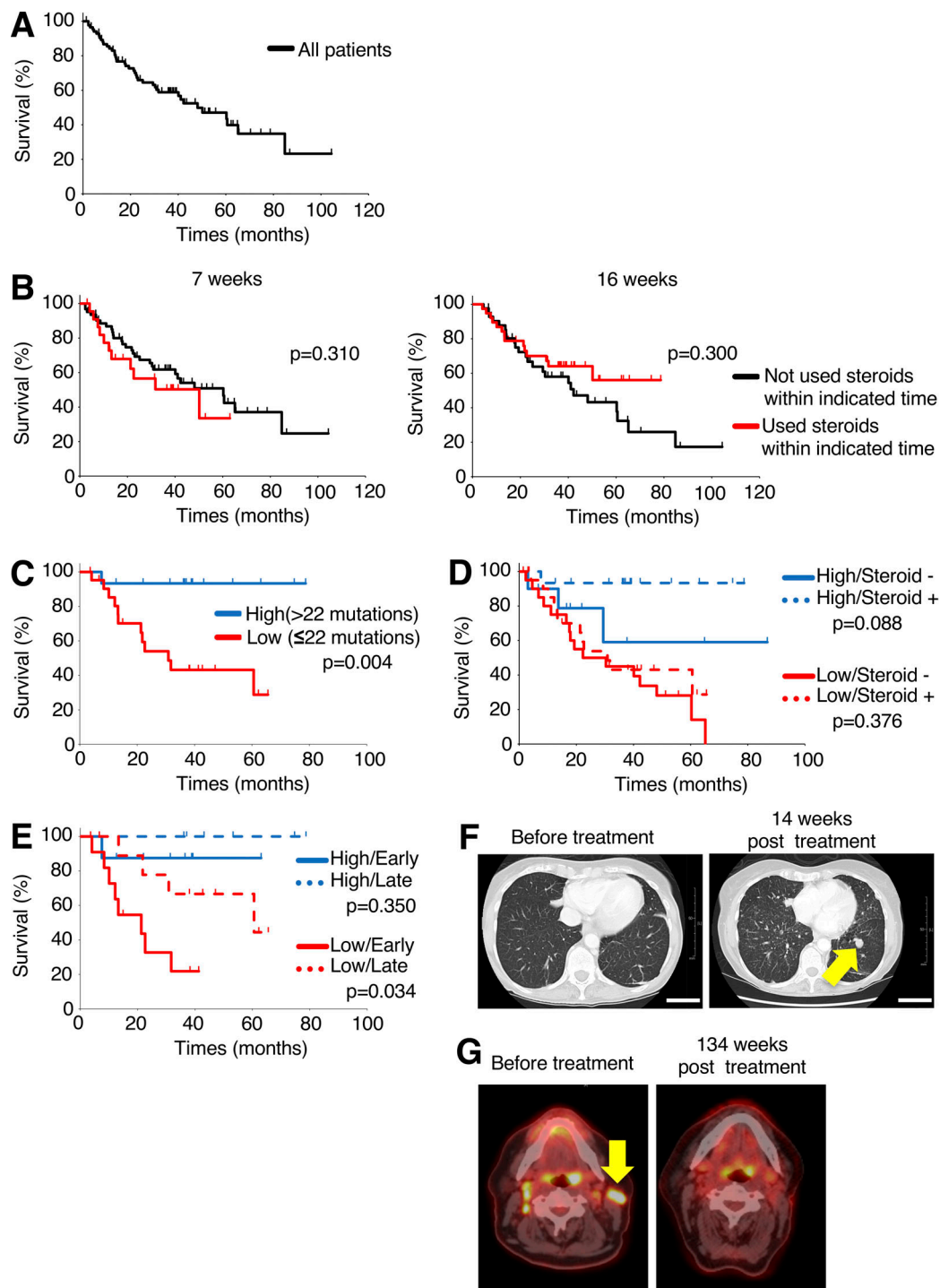


Figure 5. Low-mutation burden and early corticosteroid administration in patients treated with anti-CTLA-4 mAb are associated with poor prognosis. (A) Kaplan–Meier curve for OS of 86 malignant melanoma patients treated with anti-CTLA-4 mAb. (B) Kaplan–Meier curves for OS by corticosteroid treatment; 7 wk (used steroids, $n = 23$, did not use steroids, $n = 62$, right) and 16 wk (used steroids, $n = 38$, did not use steroids, $n = 42$, left). (C–E) Kaplan–Meier curves for OS of corticosteroid-treated patients, classified on the basis of high (>22 mutations)/low (≤ 22 mutations)–mutation burdens determined by MSK-IMPACT, a next-generation sequencing technique that can identify alterations in 468 cancer-associated genes, to identify tumor mutation burden (C); any corticosteroid administration to patients with high-/low-mutation burdens (high-mutation/used corticosteroids, $n = 15$, high-mutation/not used corticosteroids, $n = 10$, low-mutation/used corticosteroids, $n = 22$, low-mutation/not used corticosteroids, $n = 21$; D), and early (≤ 7 wk)/late (>7 wk) corticosteroid administration to patients with high-/low-mutation burdens (high-mutation/early, $n = 8$, high-mutation/late, $n = 7$, low-mutation/early, $n = 12$, low-mutation/late, $n = 10$; E). (F) Representative computed tomography scans of early corticosteroid-treated patient with low-mutation burden before (left) and 14 wk after anti-CTLA-4 mAb treatment with evidence of new and progressive pulmonary metastases (right). Scale bars, 50 mm. (G) Representative positron emission tomography images of late corticosteroid-treated patient with high-mutation burden before (left) and 134 wk after anti-CTLA-4 mAb treatment (right). Statistical analysis by log-rank test.

Female BALB/c mice and C57BL/6 mice were purchased from CLEA Japan and used at 6–10 wk of age. OT-I TCR transgenic mice were kindly provided by William R. Heath (University of Melbourne, Melbourne, Australia). All mice were maintained in a specific pathogen-free facility at the National Cancer Center (Tokyo/Chiba, Japan) and Nagoya University (Nagoya, Japan). The experimental protocol was approved by the Institutional Animal Experimental Committee at the National Cancer Center and Nagoya University.

Abs and reagents

Purified anti-CD3 ϵ (145-2C11) mAb, PerCP/Cy5.5-conjugated anti-CD3 ϵ (145-2C11) mAb, Alexa Fluor 700-conjugated anti-CD3 (17A2) mAb, Alexa Fluor 488-conjugated anti-CD3 (17A2) mAb, Brilliant Violet 510 (BV510)-conjugated anti-CD8 α (53-6.7) mAb, BV421-conjugated anti-KLRG1 (2F1/KLRG1) mAb, BV711-conjugated anti-CD127 (A7R34) mAb, PE-conjugated anti-CD69 (H1.2F3) mAb, PE-conjugated anti-phosphorylated ERK1/2 (6B8B69) mAb, BV421-conjugated anti-CD86 (GL-1) mAb, Alexa Fluor 488-conjugated anti-I-A/I-E (M5/114.15.2) mAb, Alexa Fluor 647-conjugated anti-F4/80 (BM8) mAb, PE/Cy7-conjugated anti-Ly-6G/Ly-6C (RB6-8C5) mAb, PerCP/Cy5.5-conjugated anti-CD40 (3/23) mAb, BV605-conjugated anti-CD11c (N418) mAb, BV421-conjugated anti-PD-1 (29F.1A12) mAb, PE-conjugated anti-Tim-3 (RMT3-23) mAb, and PE-conjugated anti-CD103 (2E7) mAb were purchased from BioLegend. PE-conjugated anti-phosphorylated ZAP-70 (17A/P-ZAP70) mAb, PE-conjugated anti-phosphorylated JNK (N9-66) mAb, PE-CF594-conjugated anti-CD80 (16-10A1) mAb, V500-conjugated anti-CD8 α (53-6.7) mAb, PE-conjugated anti-TNF- α (MP6-XT22) mAb, and mouse TCR V β screening panel were purchased from BD Biosciences. FITC-conjugated anti-CD8 (KT15) mAb was obtained from MBL. eFluor 780-conjugated fixable dye, FITC-conjugated anti-IFN- γ (XMG1.2) mAb, and PE/Cy7-conjugated Ki-67 (SolA15) mAb were purchased from Thermo Fisher Scientific. Anti-phosphorylated GR polyclonal Ab was purchased from Merck Millipore. Anti-phosphorylated ERK1/2 (D13.14.4E) mAb, anti-ERK1/2 (137F5) mAb, anti-phosphorylated JNK (81E11) mAb, anti-JNK polyclonal Ab, and anti- β -actin polyclonal Ab were purchased from Cell Signaling Technology. OVA peptides, SIINFEKL (N4) and SIYNFEKL (Y3), were obtained from Eurofins Genomics. NY-ESO-1 peptide, RGPESRL, and CMS5a-intAg peptide, QYIHSANVL, were obtained from Genscript. Methylprednisolone sodium succinate was purchased from Pfizer.

Ab labeling

Anti-phosphorylated GR polyclonal Ab was labeled with Zenon Rabbit IgG Labeling Kits (Thermo Fisher Scientific) according to the manufacturer's instructions.

Tumor model

Mice were inoculated subcutaneously with 2×10^6 CMS5a-NY-ESO-1 cells or 10^6 CT26-NY-ESO-1 cells in the right hind flank. Some mice then received intravenous injections of 100 μ g of anti-CTLA-4 mAb (9D9) or 200 μ g of anti-PD-L1 mAb (10F.9G2) with/without methylprednisolone at the indicated doses. In the secondary challenge experiments, 39 d after primary tumor challenge, tumor-free

mice were rechallenged subcutaneously with 10^7 CMS5a-NY-ESO-1 and parental CMS5a cells, or 5×10^6 CT26-NY-ESO-1 and parental CT26 cells. Mice were monitored twice a week and were sacrificed when tumors were >20 mm in diameter.

Surface marker and tetramer staining

After mechanical dissociation of tumors and spleens to prepare single-cell suspension, cells were stained with APC-labeled NY-ESO-1-tetramer or PE-labeled OVA-tetramer (TCMetrix) for 10 min at 37°C and further stained with various mAbs including CD3, CD8 α , CD69, KLRG1, or CD127 and with fixable viability dye. After washing, cells were analyzed with an LSR Fortessa instrument (BD Biosciences) and FlowJo software (Treestar). The Abs were used according to the manufacturer's instructions.

DC staining

After mechanical dissociation of tumor-draining lymph nodes, cells were stained with various mAbs including CD3, CD8 α , CD11c, MHC class II, CD40, CD80, and CD86 and with fixable viability dye. After washing, cells were analyzed with an LSR Fortessa instrument and FlowJo software. The Abs were used according to the manufacturer's instructions.

ELISA

DCs from draining lymph nodes in CMS5a-NY-ESO-1-bearing mice at 10 d after tumor inoculation were purified by CD11c microbeads (Miltenyi Biotec) and were stimulated with LPS (1 μ g/ml) overnight. Production of IL-12p70 in DC culture supernatants was measured by ELISA (R&D Systems) according to the manufacturer's instructions.

Stimulation of OT-I cells

Splenocytes of OT-I mice were stimulated with 1 nmol/liter N4 or Y3 peptide. 3 h after stimulation, cells were fixed using intracellular (IC) fixation buffer (Thermo Fisher Scientific), permeabilized with methanol according to the manufacturer's instructions, and stained with mAbs specific for CD3, CD8, phosphorylated ZAP-70, phosphorylated ERK1/2, or phosphorylated JNK. Phosphorylation of TCR downstream molecules was determined by flow cytometry. 7 d after stimulation, OVA tetramer⁺ cells in CD8⁺ T cells were determined by flow cytometry.

Microarray analysis

Peptide-activated OT-I cells treated with/without corticosteroid were stained with OVA tetramer and sorted with a FACSAria Fusion (BD Biosciences). The purity was confirmed to be >95%. Total RNA was isolated with the RNeasy Plus Mini Kit (Qiagen) and subjected to microarray analysis (Clariom D Assay, Mouse; Thermo Fisher Scientific). Obtained raw data were normalized by the robust multi-array average algorithm. Enriched pathways were determined using the GSEA tool available from the Broad Institute website. Hallmark gene sets were downloaded from the Molecular Signatures Database.

Extracellular flux analysis

Oxygen consumption rate (OCR) was measured with XF96 extracellular flux analyzer (Seahorse Biosciences). XF96 plates

were coated using CellTak (BD Biosciences). Peptide-activated OT-I cells treated with/without corticosteroid were seeded in XF Base Medium containing 1% FBS, 1 mmol/liter sodium pyruvate, 2 mmol/liter L-glutamine, and 10 mmol/liter glucose. The amount of FAO-associated OCR was determined by adding etomoxir (200 μ M).

FAO-associated mitochondrial membrane potential assay

After T cells in tumors were prepared from CMS5a-NY-ESO-1-bearing mice, cells were incubated in PBS containing 500 mmol/liter etomoxir for 30 min at 37°C. After continuous incubation with 400 nmol/liter Tetramethylrhodamine Methyl Ester Perchlorate (TMRE) for 30 min at 37°C, cells were stained with NY-ESO-1-tetramer, anti-CD3 mAb, anti-CD8 mAb, and fixable viability dye. Then, cells were analyzed with a flow cytometry and FlowJo software. The rate of changes in TMRE-negative cells was calculated with or without etomoxir.

Quantitative real-time PCR

High-affinity (NY-ESO-1-tetramer⁺) and low-affinity (NY-ESO-1-tetramer⁻) CD8⁺ T cells in tumors from CMS5a-NY-ESO-1-bearing mice were sorted with FACSaria Fusion. RNA was extracted using RNeasy Plus Mini Kit, and cDNA was synthesized using SuperScript VILO Master Mix (Thermo Fisher Scientific). Quantitative real-time PCR was performed with Taqman probe (Thermo Fisher Scientific) according to the manufacturer's instructions. Primers for *ACSL4*, *ACADS*, *ACADL*, *ECHS1*, and *HADH* were purchased from Applied Biosystems. 18S ribosomal RNA was used as an internal control.

Malignant melanoma patients and response assessment

We retrospectively identified patients with advanced, unresectable, or metastatic melanoma who were treated with ipilimumab monotherapy at Memorial Sloan Kettering Cancer Center between 2010 and October 2017. Of the identified patients, we selected those whose tumors were tested by MSK-IMPACT, a next-generation sequencing technique that can identify alterations in 468 cancer-associated genes, to identify tumor mutation burden. Pharmacy data and clinic notes were reviewed to identify the date and dosage of corticosteroid administration, if applicable. The blood specimens and tumor samples were collected under Memorial Sloan Kettering Cancer Center Institutional Review Board protocols 00-144 and 06-107.

Immunization and T cell assays

A total of 100 μ g NY-ESO-1 peptide or CMS5a-intAg peptide with a combined adjuvant for synergistic activation of cellular immunity (CASAC) vaccine was injected subcutaneously in both flanks of mice at day 0 and day 9. CASAC vaccine was prepared using the CpG oligodeoxynucleotide 1826 (25 μ g; Enzo Life Sciences), poly:IC (50 μ g; Merck Millipore), IFN- γ (100 ng; Miltenyi Biotec), and anti-mouse CD40 mAb (25 μ g; Biolegend) in Ribi adjuvant (100 μ l, used as per the manufacturer's instructions; Merck Millipore). Draining lymph nodes from immunized mice were mechanically dissociated to prepare single-cell suspensions and subjected to staining of

APC-labeled NY-ESO-1 or PE-labeled CMS5a-intAg dextramer (Immudex), anti-CD3 mAb, and anti-CD8 mAb. After washing, CD3⁺CD8⁺NY-ESO-1 or CMS5a-intAg dextramer-positive cells were sorted with a FACSaria III instrument (BD Biosciences). Sorted cells were cultured with P1.HTR cells pulsed with 1 nmol/liter NY-ESO-1 or CMS5a-intAg peptide with/without corticosteroids (25 ng/ml). 3 h after stimulation, cells were fixed using IC fixation buffer, permeabilized with methanol according to the manufacturer's instructions, and stained with Abs specific for CD3, CD8, phosphorylated ZAP-70, phosphorylated ERK1/2, or GR. Phosphorylation of these molecules was determined by flow cytometry.

Immunoblotting

Splenic CD8⁺ T cells were isolated using a CD8⁺ T cell isolation kit (Miltenyi Biotec), and purity was confirmed to be >95%. Purified CD8⁺ T cells were rested in RPMI 1640 containing 1% FBS for 30 min at 37°C. Cells were stimulated with titrated doses of anti-CD3 ϵ mAb and followed by goat anti-Armenian hamster IgG cross-linking for 5 min at 37°C. After centrifugation, cells were lysed in NP-40 cell lysis buffer (Thermo Fisher Scientific) containing protease and phosphatase inhibitors. All lysates were separated by SDS-PAGE and transferred onto polyvinylidene difluoride membranes. Proteins were detected by incubation with primary Abs, specific for phosphorylated ERK1/2, ERK1/2, phosphorylated JNK, JNK, phosphorylated GR, GR, or β -actin followed by horseradish peroxidase-linked secondary Ab. Images were obtained using an Amersham Imager 600 (GE Healthcare), and bands were quantified with ImageJ software (National Institutes of Health).

TCR repertoire analysis

After mechanical dissociation of tumor tissue from anti-CTLA-4-treated mice, cells were stained with various mAbs including APC-labeled NY-ESO-1-dextramer, anti-CD3 mAb, anti-CD8 mAb, and anti-CD69 mAb. After washing, CD3⁺CD8⁺NY-ESO-1-dextramer⁻CD69⁺ (from CMS5a-NY-ESO-1-bearing mice) or CD3⁺CD8⁺CD69⁺ (from CMS5a-bearing mice) cells were sorted with FACSaria III instrument. RNA was extracted using the RNeasy Plus Micro Kit, and cDNA libraries were generated using a SMARTer Mouse TCR a/b Profiling Kit (TaKaRa Bio). Sequencing and TCR repertoire analysis were performed by TaKaRa Bio.

ELISPOT assay

CD8⁺ T cells were purified from draining lymph nodes of mice immunized with NY-ESO-1 or CMS5a-intAg peptide using CD8 Microbeads (Miltenyi Biotec). CD90-depleted splenocytes were purified using CD90.2 Microbeads (Miltenyi Biotec). CD8⁺ T cells (10⁵ cells) were cultured for 22 h with the CD90-negative cells (2 \times 10⁵ cells) pulsed with the indicated peptides in MultiScreen plate (Merck Millipore) coated with rat anti-mouse IFN- γ mAb (R4-6A2; BD Biosciences). IFN- γ spots were developed using biotinylated rat anti-mouse IFN- γ mAb (XMG1.2; BD Biosciences), streptavidin-alkaline phosphatase-conjugate (Sigma-Aldrich), and alkaline phosphatase substrate (Sigma-Aldrich), and subsequently counted.

Statistical analysis

Statistical differences between groups were determined with the GraphPad Prism 6 software using Student's *t* test, one-way ANOVA with post hoc Dunnett's test, or log-rank test. *P* values <0.05 were considered statistically significant.

Data availability statement

The data that support the findings of this study are available from the corresponding authors upon reasonable request. The microarray data have been deposited in GEO under accession no. GSE136236.

Online supplemental material

Fig. S1 shows the impairment of low-affinity memory T cell differentiation. Fig. S2 shows low-affinity TCR in CMS5a-intAg-specific CD8⁺ T cells. Fig. S3 shows selective impairment of FAO in low-affinity but not high-affinity memory T cells by corticosteroid treatment.

Acknowledgments

We thank D. Ha, Y. Tada, M. Takemura, and K. Teshima for technical assistance and special animal care by the Division of Experimental Animals, Nagoya University Graduate School of Medicine.

This study was supported by the Ministry of Education, Culture, Sports, Science and Technology of Japan (Grants-in-Aid for Scientific Research S grant no. 17H06162 to H. Nishikawa and Challenging Exploratory Research grant no. 16K15551 to H. Nishikawa), by the National Cancer Center Research and Development Fund (no. 28-A-7 and 31-A-7 to H. Nishikawa), and by the Naito Foundation. This study was funded in part through the National Institutes of Health/National Cancer Institute Cancer Center Support Grant (no. P30 CA008748 to J.D. Wolchok). A.B. Warner is supported by a grant from the Conquer Cancer Foundation of American Society of Clinical Oncology.

A. Tokunaga is an employee of Kyowa Kirin. Y. Togashi received honoraria and research grant from Ono Pharmaceutical Company and Bristol-Myers Squibb. J.D. Wolchok lists the following interests: consultant, Adaptive Biotech, Advaxis, Amgen, Apricity, Array BioPharma, Ascentage Pharma, Astellas, Beigene, Bristol-Myers Squibb, Celgene, Chugai, Elucida, Eli Lilly, F Star, Genentech, Imvaq, Kleo Pharma, MedImmune, Merck, Neon Therapeutics, Ono Pharmaceutical, Polaris Pharma, Polynoma, Psioxus, Puretech, Recepta, Trienza, Sellas Life Sciences, Seramatrix, Surface Oncology, and Syndax; research support: Bristol-Myers Squibb, Medimmune, Merck Pharmaceuticals, and Genentech; equity in Potenza Therapeutics, Tizona Pharmaceuticals, Adaptive Biotechnologies, Elucida, Imvaq, Beigene, and Trieza. H. Nishikawa received honoraria and grants from Ono Pharmaceutical, Bristol-Myers Squibb, and Chugai Pharmaceutical, and grants from Taiho Pharmaceutical, Daiichi-Sankyo, Kyowa Kirin, Zenyaku Kogyo, Astellas Pharmaceutical, Sysmex, and BD Japan outside of this study. The other authors declare no competing financial interests.

Author contributions: J.D. Wolchok and H. Nishikawa designed the research; A. Tokunaga, D. Sugiyama, Y. Maeda, S. Ito,

Y. Togashi, and C. Sakai performed experiments; A.B. Warner obtained clinical data; A. Tokunaga, D. Sugiyama, Y. Maeda, A.B. Warner, K.S. Panageas, J.D. Wolchok, and H. Nishikawa analyzed data; and A. Tokunaga, A.B. Warner, J.D. Wolchok, and H. Nishikawa wrote the paper.

Submitted: 24 April 2019

Revised: 12 August 2019

Accepted: 3 September 2019

References

- Ashwell, J.D., F.W. Lu, and M.S. Vacchio. 2000. Glucocorticoids in T cell development and function. *Annu. Rev. Immunol.* 18:309-345. <https://doi.org/10.1146/annurev.immunol.18.1.309>
- Barnes, P.J., and I.M. Adcock. 2009. Glucocorticoid resistance in inflammatory diseases. *Lancet.* 373:1905-1917. [https://doi.org/10.1016/S0140-6736\(09\)60326-3](https://doi.org/10.1016/S0140-6736(09)60326-3)
- Butler, M.O., P. Friedlander, M.I. Milstein, M.M. Mooney, G. Metzler, A.P. Murray, M. Tanaka, A. Berezovskaya, O. Imataki, L. Drury, et al. 2011. Establishment of antitumor memory in humans using in vitro-educated CD8⁺ T cells. *Sci. Transl. Med.* 3. <https://doi.org/10.1126/scitranslmed.3002207>
- Callahan, M.K., M.A. Postow, and J.D. Wolchok. 2016. Targeting T Cell Co-receptors for Cancer Therapy. *Immunity.* 44:1069-1078. <https://doi.org/10.1016/j.immuni.2016.04.023>
- Chen, D.S., and I. Mellman. 2017. Elements of cancer immunity and the cancer-immune set point. *Nature.* 541:321-330. <https://doi.org/10.1038/nature21349>
- Curiel, T.J., S. Wei, H. Dong, X. Alvarez, P. Cheng, P. Mottram, R. Krzysiek, K.L. Knutson, B. Daniel, M.C. Zimmermann, et al. 2003. Blockade of B7-H1 improves myeloid dendritic cell-mediated antitumor immunity. *Nat. Med.* 9:562-567. <https://doi.org/10.1038/nm863>
- Esensten, J.H., Y.A. Helou, G. Chopra, A. Weiss, and J.A. Bluestone. 2016. CD28 Costimulation: From Mechanism to Therapy. *Immunity.* 44: 973-988. <https://doi.org/10.1016/j.immuni.2016.04.020>
- Feng, S., J. Coward, E. McCaffrey, J. Coucher, P. Kalokerinos, and K. O'Byrne. 2017. Pembrolizumab-Induced Encephalopathy: A Review of Neurological Toxicities with Immune Checkpoint Inhibitors. *J. Thorac. Oncol.* 12:1626-1635. <https://doi.org/10.1016/j.jtho.2017.08.007>
- Freeman, G.J., A.J. Long, Y. Iwai, K. Bourque, T. Chernova, H. Nishimura, L.J. Fitz, N. Malenkovich, T. Okazaki, M.C. Byrne, et al. 2000. Engagement of the PD-1 immunoinhibitory receptor by a novel B7 family member leads to negative regulation of lymphocyte activation. *J. Exp. Med.* 192: 1027-1034. <https://doi.org/10.1084/jem.192.7.1027>
- Griswold, D.P., and T.H. Corbett. 1975. A colon tumor model for anticancer agent evaluation. *Cancer.* 36(6 Suppl):2441-2444.
- Hanson, H.L., D.L. Donermeyer, H. Ikeda, J.M. White, V. Shankaran, L.J. Old, H. Shiku, R.D. Schreiber, and P.M. Allen. 2000. Eradication of established tumors by CD8⁺ T cell adoptive immunotherapy. *Immunity.* 13: 265-276. [https://doi.org/10.1016/S1074-7613\(00\)00026-1](https://doi.org/10.1016/S1074-7613(00)00026-1)
- Hildner, K., B.T. Edelson, W.E. Purtha, M. Diamond, H. Matsushita, M. Kohyama, B. Calderon, B.U. Schraml, E.R. Unanue, M.S. Diamond, et al. 2008. Batf3 deficiency reveals a critical role for CD8α⁺ dendritic cells in cytotoxic T cell immunity. *Science.* 322:1097-1100. <https://doi.org/10.1126/science.1164206>
- Hodi, F.S., S.J. O'Day, D.F. McDermott, R.W. Weber, J.A. Sosman, J.B. Haanen, R. Gonzalez, C. Robert, D. Schadendorf, J.C. Hassel, et al. 2010. Improved survival with ipilimumab in patients with metastatic melanoma. *N. Engl. J. Med.* 363:711-723. <https://doi.org/10.1056/NEJMoa1003466>
- Horvat, T.Z., N.G. Adel, T.O. Dang, P. Momtaz, M.A. Postow, M.K. Callahan, R.D. Carvajal, M.A. Dickson, S.P. D'Angelo, K.M. Woo, et al. 2015. Immune-Related Adverse Events, Need for Systemic Immunosuppression, and Effects on Survival and Time to Treatment Failure in Patients With Melanoma Treated With Ipilimumab at Memorial Sloan Kettering Cancer Center. *J. Clin. Oncol.* 33:3193-3198. <https://doi.org/10.1200/JCO.2015.60.8448>
- Hui, E., J. Cheung, J. Zhu, X. Su, M.J. Taylor, H.A. Wallweber, D.K. Sasmal, J. Huang, J.M. Kim, I. Mellman, and R.D. Vale. 2017. T cell costimulatory receptor CD28 is a primary target for PD-1-mediated inhibition. *Science.* 355:1428-1433. <https://doi.org/10.1126/science.aaf1292>

- Joshi, N.S., W. Cui, A. Chandele, H.K. Lee, D.R. Urso, J. Hagman, L. Gapin, and S.M. Kaech. 2007. Inflammation directs memory precursor and short-lived effector CD8⁺ T cell fates via the graded expression of T-bet transcription factor. *Immunity*. 27:281–295. <https://doi.org/10.1016/j.immuni.2007.07.010>
- June, C.H., J.T. Warshauer, and J.A. Bluestone. 2017. Is autoimmunity the Achilles' heel of cancer immunotherapy? *Nat. Med.* 23:540–547. <https://doi.org/10.1038/nm.4321>
- Kamphorst, A.O., A. Wieland, T. Nasti, S. Yang, R. Zhang, D.L. Barber, B.T. Konieczny, C.Z. Daugherty, L. Koenig, K. Yu, et al. 2017. Rescue of exhausted CD8 T cells by PD-1-targeted therapies is CD28-dependent. *Science*. 355:1423–1427. <https://doi.org/10.1126/science.aaf0683>
- Khalil, D.N., E.L. Smith, R.J. Brentjens, and J.D. Wolchok. 2016. The future of cancer treatment: immunomodulation, CARs and combination immunotherapy. *Nat. Rev. Clin. Oncol.* 13:273–290. <https://doi.org/10.1038/nrclinonc.2016.25>
- Ki, S.H., I.J. Cho, D.W. Choi, and S.G. Kim. 2005. Glucocorticoid receptor (GR)-associated SMRT binding to C/EBPbeta TAD and Nrf2 Neh4/5: role of SMRT recruited to GR in GSTA2 gene repression. *Mol. Cell. Biol.* 25:4150–4165. <https://doi.org/10.1128/MCB.25.10.4150-4165.2005>
- Knudson, K.M., N.P. Goplen, C.A. Cunningham, M.A. Daniels, and E. Teixeiro. 2013. Low-affinity T cells are programmed to maintain normal primary responses but are impaired in their recall to low-affinity ligands. *Cell Reports*. 4:554–565. <https://doi.org/10.1016/j.celrep.2013.07.008>
- Leach, D.R., M.F. Krummel, and J.P. Allison. 1996. Enhancement of antitumor immunity by CTLA-4 blockade. *Science*. 271:1734–1736. <https://doi.org/10.1126/science.271.5256.1734>
- Lin, H., S. Wei, E.M. Hurt, M.D. Green, L. Zhao, L. Vatan, W. Szeliga, R. Herbst, P.W. Harms, L.A. Fecher, et al. 2018. Host expression of PD-L1 determines efficacy of PD-L1 pathway blockade-mediated tumor regression. *J. Clin. Invest.* 128:805–815. <https://doi.org/10.1172/JCI96113>
- Löwenberg, M., A.P. Verhaar, G.R. van den Brink, and D.W. Hommes. 2007. Glucocorticoid signaling: a nongenomic mechanism for T-cell immunosuppression. *Trends Mol. Med.* 13:158–163. <https://doi.org/10.1016/j.molmed.2007.02.001>
- Mitsui, J., H. Nishikawa, D. Muraoka, L. Wang, T. Noguchi, E. Sato, S. Kondo, J.P. Allison, S. Sakaguchi, L.J. Old, et al. 2010. Two distinct mechanisms of augmented antitumor activity by modulation of immunostimulatory/inhibitory signals. *Clin. Cancer Res.* 16:2781–2791. <https://doi.org/10.1158/1078-0432.CCR-09-3243>
- Nishikawa, H., E. Sato, G. Briones, L.M. Chen, M. Matsuo, Y. Nagata, G. Ritter, E. Jäger, H. Nomura, S. Kondo, et al. 2006. In vivo antigen delivery by a *Salmonella typhimurium* type III secretion system for therapeutic cancer vaccines. *J. Clin. Invest.* 116:1946–1954. <https://doi.org/10.1172/JCI28045>
- Palucka, K., and J. Banchereau. 2016. Diversity and collaboration for effective immunotherapy. *Nat. Med.* 22:1390–1391. <https://doi.org/10.1038/nm.4249>
- Pearce, E.L., M.C. Walsh, P.J. Cejas, G.M. Harms, H. Shen, L.S. Wang, R.G. Jones, and Y. Choi. 2009. Enhancing CD8 T-cell memory by modulating fatty acid metabolism. *Nature*. 460:103–107. <https://doi.org/10.1038/nature08097>
- Phuc Le, P., J.R. Friedman, J. Schug, J.E. Brestelli, J.B. Parker, I.M. Bochkis, and K.H. Kaestner. 2005. Glucocorticoid receptor-dependent gene regulatory networks. *PLoS Genet.* 1:e16. <https://doi.org/10.1371/journal.pgen.0010016>
- Pitt, J.M., M. Vétizou, R. Daillère, M.P. Roberti, T. Yamazaki, B. Routy, P. Lepage, I.G. Boneca, M. Chamillard, G. Kroemer, and L. Zitvogel. 2016. Resistance Mechanisms to Immune-Checkpoint Blockade in Cancer: Tumor-Intrinsic and -Extrinsic Factors. *Immunity*. 44:1255–1269. <https://doi.org/10.1016/j.immuni.2016.06.001>
- Raud, B., D.G. Roy, A.S. Divakaruni, T.N. Tarasenko, R. Franke, E.H. Ma, B. Samborska, W.Y. Hsieh, A.H. Wong, P. Stüve, et al. 2018. Etomoxir Actions on Regulatory and Memory T Cells Are Independent of Cpt1a-Mediated Fatty Acid Oxidation. *Cell Metab.* 28:504–515.e7. <https://doi.org/10.1016/j.cmet.2018.06.002>
- Scholer, A., S. Hugues, A. Boissonnas, L. Fetler, and S. Amigorena. 2008. Intercellular adhesion molecule-1-dependent stable interactions between T cells and dendritic cells determine CD8⁺ T cell memory. *Immunity*. 28:258–270. <https://doi.org/10.1016/j.immuni.2007.12.016>
- Van den Eynde, B.J., and P. van der Bruggen. 1997. T cell defined tumor antigens. *Curr. Opin. Immunol.* 9:684–693. [https://doi.org/10.1016/S0952-7915\(97\)80050-7](https://doi.org/10.1016/S0952-7915(97)80050-7)
- van der Windt, G.J., B. Everts, C.H. Chang, J.D. Curtis, T.C. Freitas, E. Amiel, E.J. Pearce, and E.L. Pearce. 2012. Mitochondrial respiratory capacity is a critical regulator of CD8⁺ T cell memory development. *Immunity*. 36:68–78. <https://doi.org/10.1016/j.immuni.2011.12.007>
- Wang, H., T.H. Peiris, A. Mowery, J. Le Lay, Y. Gao, and L.E. Greenbaum. 2008. CCAAT/enhancer binding protein-beta is a transcriptional regulator of peroxisome-proliferator-activated receptor-gamma coactivator-alpha in the regenerating liver. *Mol. Endocrinol.* 22:1596–1605. <https://doi.org/10.1210/me.2007-0388>
- Wang, J.C., M.K. Derynck, D.F. Nonaka, D.B. Khodabakhsh, C. Haqq, and K.R. Yamamoto. 2004. Chromatin immunoprecipitation (ChIP) scanning identifies primary glucocorticoid receptor target genes. *Proc. Natl. Acad. Sci. USA*. 101:15603–15608. <https://doi.org/10.1073/pnas.0407008101>
- Wherry, E.J., and M. Kurachi. 2015. Molecular and cellular insights into T cell exhaustion. *Nat. Rev. Immunol.* 15:486–499. <https://doi.org/10.1038/nri3862>
- Wing, K., and S. Sakaguchi. 2010. Regulatory T cells exert checks and balances on self tolerance and autoimmunity. *Nat. Immunol.* 11:7–13. <https://doi.org/10.1038/ni.1818>
- Wolchok, J.D., V. Chiarion-Sileni, R. Gonzalez, P. Rutkowski, J.J. Grob, C.L. Cowey, C.D. Lao, J. Wagstaff, D. Schadendorf, P.F. Ferrucci, et al. 2017. Overall Survival with Combined Nivolumab and Ipilimumab in Advanced Melanoma. *N. Engl. J. Med.* 377:1345–1356. <https://doi.org/10.1056/NEJMoa1709684>
- Yarchoan, M., B.A. Johnson III, E.R. Lutz, D.A. Laheru, and E.M. Jaffee. 2017. Targeting neoantigens to augment antitumor immunity. *Nat. Rev. Cancer*. 17:209–222. <https://doi.org/10.1038/nrc.2016.154>
- Zehn, D., S.Y. Lee, and M.J. Bevan. 2009. Complete but curtailed T-cell response to very low-affinity antigen. *Nature*. 458:211–214. <https://doi.org/10.1038/nature07657>